Available online at www.sciencedirect.com
SCIENCE DIRECT
International Journal of Heat and Mass Transfer 49 (2006) 1287–1298
International Journal of HEAT and MASS TRANSFER
www.elsevier.com/locate/ijhmt

Experimental investigations on showerhead cooling on a blunt body

C. Falcoz [a], B. Weigand [b,*], P. Ott [a]

[a] Ecole Polytechnique Fédérale de Lausanne (EPFL), Laboratoire de Thermique Appliquée et de Turbomachines (LTT), 1015 Lausanne, Switzerland
[b] Institut für Thermodynamik der Luft- und Raumfahrt (ITLR), Stuttgart University, Pfaffenwaldring 31, 70569 Stuttgart, Germany

Received 15 December 2004; received in revised form 31 August 2005
Available online 6 December 2005

Abstract

In modern gas turbines, the turbine airfoil leading edge is currently protected from the hot gases by specific film cooling schemes, so-called showerhead cooling. The present paper shows an experimental study of different showerhead cooling geometries on a blunt body. For these tests, TLC (thermochromatic liquid crystals) have been used for measuring the film cooling performance and the heat transfer. Detailed experimental results for the aerodynamics, the film cooling effectiveness and the heat transfer enhancement are presented for different film cooling geometries.

1. Introduction

In modern gas turbine designs, there is a strong desire to increase the inlet hot-gas temperature of the turbine. This would lead to much higher blade temperatures than the maximum allowable metal temperature of the gas turbine blades. In order to protect the turbine blades from melting, the blades need extensive cooling by internal air flow. Usually a combination of internal convective cooling and external film cooling is employed. The cooling designs of these parts have to be highly efficient, because of the fact that a larger cooling mass flow rate degrades the thermal efficiency of the thermodynamic cycle of the gas turbine. This is especially true for the application of film cooling, where a protective film of cold air is spread around the blade and large cooling mass flows are required. Because of the importance of film cooling for turbine blade design, the subject has been studied extensively over the past 35 years. Several review articles on film cooling are published on this subject [1–3]. Showerhead cooling is much more complicated than normal film cooling on a profile, because of the strong curvature effects of the blade profile. The showerhead cooling is used in order to protect the stagnation point area of a first vane or a first blade against the extremely high gas temperatures. In contrast to film cooling on a turbine blade, the coolant flow out of the holes in the nose of the profile can hardly form a good cooling film around the profile. On the other side, the coolant flow takes heat from the blade material while flowing through the relatively long coolant holes in the nose of the profile. To extend the coolant holes in length, mostly these coolant holes are inclined radially. Because of the above cited features of showerhead cooling, the cooling of the leading edge of an airfoil by the showerhead cooling contents the external film cooling, the internal cooling in the coolant holes as well as the cooling inside the main coolant channel inside the blade. In order to evaluate the performance of showerhead cooling schemes, all three aspects of showerhead cooling have to be addressed. This is the aim of the present and a companion paper [18]. The present paper investigates the external film cooling aspects alone, whereas the companion paper [18] shows the evaluation of the global performance of the showerhead cooling model by using 2D and 3D finite element models (FEM).

In order to test the influence of the different parameters acting on leading edge film cooling, several studies were conducted in the past on curved surfaces in order to simulate the flow characteristics of the stagnation region. Different methods were reported in the literature to model the

* Corresponding author. Tel.: +49 711 685 3590; fax: +49 711 685 2317.
E-mail address: bw@itlr.uni-stuttgart.de (B. Weigand).

0017-9310/$ - see front matter © 2005 Elsevier Ltd. All rights reserved.
doi:10.1016/j.ijheatmasstransfer.2005.10.012

Nomenclature

a	sonic velocity, $\sqrt{\kappa RT}$ [m/s]
c_p, c_v	specific heat at constant pressure and constant volume [J/(kg K)]
CD	discharge coefficient, CD $= \dot{m}/\dot{m}_{\text{ideal}}$ [–]
D	leading edge cylinder diameter [m]
d	cooling hole diameter [m]
DR	coolant-to-mainstream density ratio, DR $= \rho_c/\rho_g = G^2/I$ [–]
G	blowing ratio, $G = \rho_c u_c/\rho_g u_\infty$, referred to hole entrance [–]
h	heat transfer coefficient [W/(m^2 K)]
I	momentum flux ratio, $I = \rho_c u_c^2/\rho_g u_\infty^2$, ref. to hole entrance [–]
k	thermal conductivity [W/(m K)]
M	approach Mach number, $M = u_\infty/a$ [–]
$\dot{m}$	massflow rate [kg/s]
$\dot{m}_{\text{ideal}}$	ideal mass flow based on isentropic 1D flow conditions [kg/s]
Nu	Nusselt number, $Nu = hD/k$ [–]
p	pressure [Pa]
p	pitch or spanwise spacing between holes in one row [m]
Re_D	Reynolds number, $Re = \rho u_\infty D/\mu$ [–]
s	surface distance from the stagnation point [m]
t	time [s]
T	temperature [°C], [K]
Tu	free-stream turbulence intensity [%]
u	velocity [m/s]
u_∞	approach velocity to blunt body [m/s]

Greek symbols

α	thermal diffusivity, $\alpha = k/(\rho c_p)$ [m^2/s]
β	spanwise inclination angle to surface [°]
γ	row exit location angle measured from stagnation line [°]
η	film cooling effectiveness, $\eta = (T_{\text{aw}} - T_{\text{rg}})/(T_{\text{tc}} - T_{\text{tg}})$ [–]
φ	streamwise inclination angle [°]
κ	isentropic exponent, $\kappa = c_p/c_v$ [–]
μ	dynamic viscosity [Ns/m^2]
θ	angle starting from the stagnation line [°]
ρ	density [kg/m^3]

Subscripts

c	coolant
g	hot gas
r	recovery conditions
t	total conditions
w, aw	wall, adiabatic wall

leading edge region. In many cases, the airfoil leading edge was simulated using a cylinder in cross-flow. Another alternative consists of placing a tailboard at the rear of the cylinder to reduce the wake effects on the upstream heat transfer. Yet another approximation, which was also widely used by researchers, consists of modeling the leading edge region using a blunt body with a semi-circular or elliptical leading edge and a flat afterbody. This has the advantage that downstream wake effects will not influence the leading edge film cooling performance and that transition effects comparable to real gas turbine blades occur. Finally, a somewhat different approach to the problem consists of investigating film cooling performance on a large-scale model of a typical turbine vane. Some of the early work on leading edge film cooling was done by Hanus and L'Ecuyer [4]. They conducted experiments on a scaled model of a turbine vane equipped with a single row of spanwise-angled holes. Some years later, Luckey and L'Ecuyer [5] simulated the airfoil leading edge as a cylinder in cross-flow with several rows of film cooling holes. They studied the influence of the blowing ratio, the injection location relative to the stagnation point, as well as the effect of multiple rows of cooling holes. The measurements showed that the film cooling performance depends strongly on the injection geometry and the coolant injection rate. Later, Wadia and Nealy [6] conducted experiments in a wind tunnel on several stainless steel cylindrical models. They compared the effects of different spanwise injection angles ($\beta = 20°$, 30°, 45°, 90°) on the leading edge film cooling effectiveness for various mainstream and coolant flow conditions. The experiments suggested that the film cooling effectiveness was primarily influenced by the inclination of the injection holes: shallower angles provided significantly increased film cooling effectiveness. Mick and Mayle [7] investigated the film cooling effectiveness and heat transfer coefficient within and downstream of three rows of cooling holes ($\gamma = \pm 15°/+44°$). Tests were performed using a blunt body with a cylindrical leading edge and a flat afterbody. Adopting the same leading edge model, Mehendale and Han [8] studied the effects of the blowing ratio (from $G = 0.4$ to 1.2) and the free-stream turbulence intensity (Tu = 0.75%, 9.67%, 12.9%) downstream of two staggered rows of holes located at ±15° and ±40° from the stagnation line. Following this work, Ou et al. [9] experimentally determined the effect of the film hole row location on the leading edge film cooling under high mainstream turbulence conditions (Tu = 9.67%). Two locations of film injection cooling holes, located only at ±15° or ±40°, were studied and compared to the four-row configuration reported by Mehendale and Han [8]. The results showed that the mainstream turbulence effect was more severe for the ±15° one-row injection than for the ±40° one-row injection. The latter produced higher effectiveness and lower surface heat load. Hoffs et al. [10] conducted film

cooling effectiveness and heat transfer investigations in a free jet test facility on film-cooled cylindrical models. A three-row ($\gamma = -21°/0°/+21°$) and a four-row ($\gamma = \pm 7°/\pm 21°$) configuration were chosen to study the cooling behavior at zero and off-design incidences. Ekkad et al. [11] focused on the effects of the coolant blowing ratio, higher coolant density and higher free stream turbulence intensity. Tests were done in a low-speed wind tunnel on a cylindrical model with two rows of cooling holes distributed symmetrically around the stagnation line ($\gamma = \pm 15°$). More recently, Reiss and Bölcs [12] examined the influence of the cooling hole geometry on film cooling performance. The authors found that, for a given coolant consumption, fan-shaped holes increased film cooling performance due to a better lateral film coverage, and a reduced tendency of "jet lift off" at high blowing rates.

As it can be seen from the literature survey given above, quite a lot of different configurations for showerhead cooling have been studied in the past. However, most of the studies have been derived under rather ideal conditions (e.g. low turbulence level, circular cylinder...) which make it difficult to use these data for real showerhead designs. On the other hand the film cooling on the leading edge of a blunt body has the advantage that realistic transition effects can be taken into account, whereas the external flow field might be fully symmetric and two-dimensional around the blunt body. Furthermore, hole geometries are sought for the leading edge cooling, which have values of the discharge coefficient (CD), which are insensitive to the pressure ratio which is applied across the coolant holes. Therefore, the present paper focuses on detailed aerodynamic and heat transfer measurements for three different hole shapes for a blunt body configuration. High turbulence levels are taken into account for these measurements.

2. Experimental setup and experiments

2.1. Experimental apparatus and test model

The present experiments for showerhead film cooling have been carried out in a linear cascade test facility. The linear test stand belongs to a network of test facilities at EPFL. Air is supplied to the network on a continuous basis by a four-stage centrifugal compressor. This compressor, driven by an electric motor at a constant speed of 9500 rpm, has a maximum pressure ratio of 3.5 and a maximum flow rate of 12 kg/s. At peak level operation, the motor consumes approximately 2.2 MW. Within the test facilities, the flow conditions are regulated using a compressor inlet valve in combination with a main air bypass valve. The flow temperature is controlled by an air/water heat exchanger.

2.1.1. Linear cascade

The original configuration of the linear test facility has been adapted for measurements on the blunt body models. Fig. 1 shows the wind tunnel holding the blunt body. The incoming flow enters the test section from the top, is directed by two sidewalls, and exits the test section at the bottom of the channel. Straight sidewalls were used in the present study, resulting in a perfect two-dimensional flow field. Increased turbulence intensity Tu of about 10% in

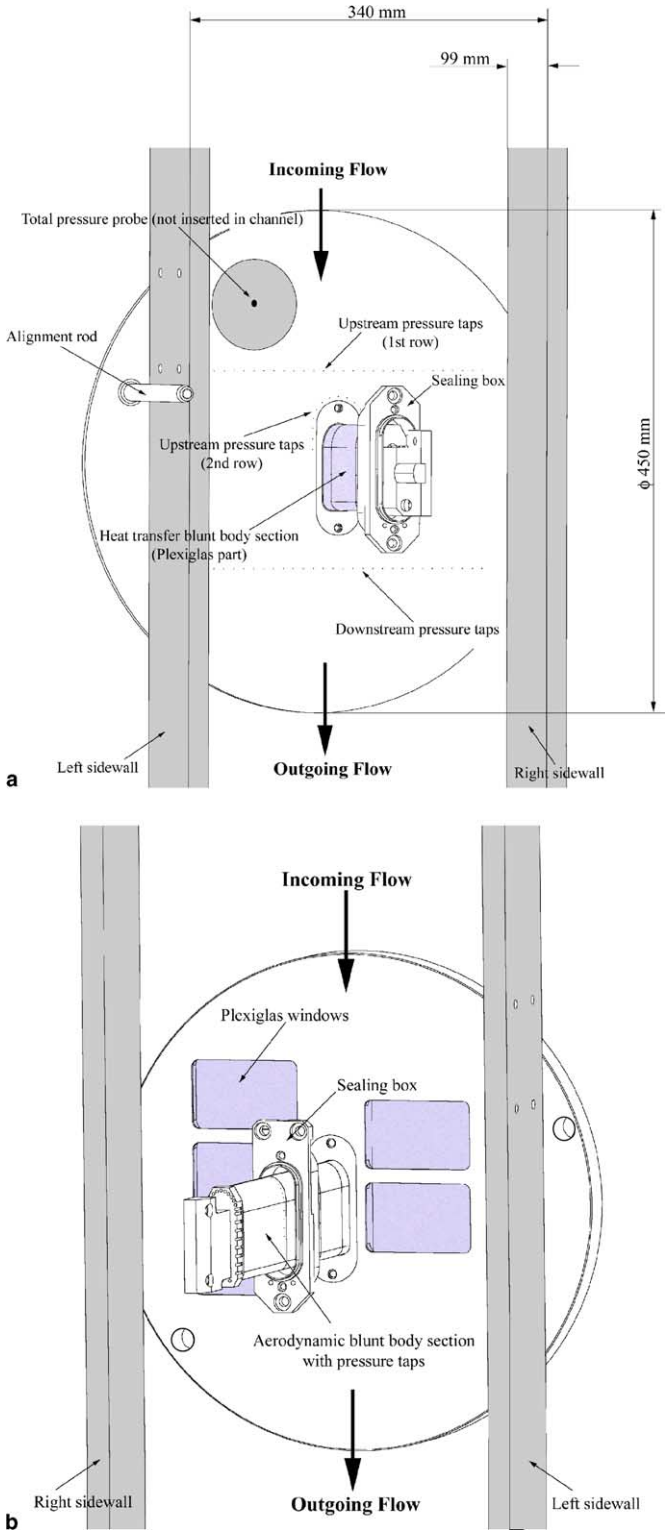

Fig. 1. Instrumented test section (1a view of heat transfer side and 1b view of aerodynamic side).

the channel is obtained by superposition of a square bar-type turbulence grid and a perforated plate inserted upstream of the test section. A removable total pressure probe is located five leading edge diameters upstream of the stagnation region of the blunt body. Retrieving the probe automatically before the insertion of the liquid crystals coated section eliminates its potential influence on heat transfer measurements. In addition, the inlet settling chamber of the test facility is equipped with a thermocouple to measure the inlet total temperature. The blunt body is mounted on rails, and can be removed from the main flow for preconditioning or re-inserted for transient tests. In its initial position, the flow and the blunt body temperature are adjusted to the desired conditions. The blunt body is then rapidly inserted by a pneumatic cylinder through the sidewalls of the test facility into the flow to start the transient experiments. Insertion time is less than 0.1 s (see e.g. [14] for a more detailed explanation).

2.1.2. Test models

The test model is a blunt body with an elliptical leading edge profile. This particular profile was chosen based on theoretical considerations, and taking into account the existing experimental hardware. In order to avoid boundary layer separation due to a step in surface curvature, the front shape of the model was designed as a Cassini curve [13]. The edges were also rounded at the rear of the model avoiding the formation of vortices. The 3D-test model, manufactured in Plexiglas, is an exchangeable part of the mobile assembly (Fig. 2). The span of this test model is 135 mm. Fig. 2b shows also some of the important geometric dimensions of the blunt body. For film-cooled configurations, most of this length is used to hold the holes pattern. Fig. 3 shows the different film cooling geometries used for the blunt body geometry. Modern configurations of diffusing holes were considered in addition to classical cylindrical holes. Configurations SHG2 and SHG3 use the same cooling arrangement in terms of hole diameter, row number, hole spacing, and inclination angles, but with modified hole exits. As shown in Fig. 3, shaped holes modify the effective exit area. The showerhead Geometry SHG2 illustrates a conical portion with a 1.8° open angle creating a diffuser of 4 hole diameters deep. The effective surface area of the hole exits is therefore increased by a factor of 1.6 compared to the cylindrical holes. The exit of the forward-diffused holes (SHG3) is opened with a 2.9° forward expansion angle over a depth of approximately 4 hole diameters. The effective surface area of the exits is therefore increased by a factor of 1.35 compared to the cylindrical holes. The geometrical data are given in Table 1.

2.1.3. Instrumentation

The test section was built up from the existing Linear Cascade ([14,15]) at EPFL and redesigned for the new geometry (blunt body) in such a manner that easy and rapid exchange of relevant parts was possible. An illustration of the test facility is provided in Fig. 1. In both figures, one sidewall—either the one situated on the heat transfer

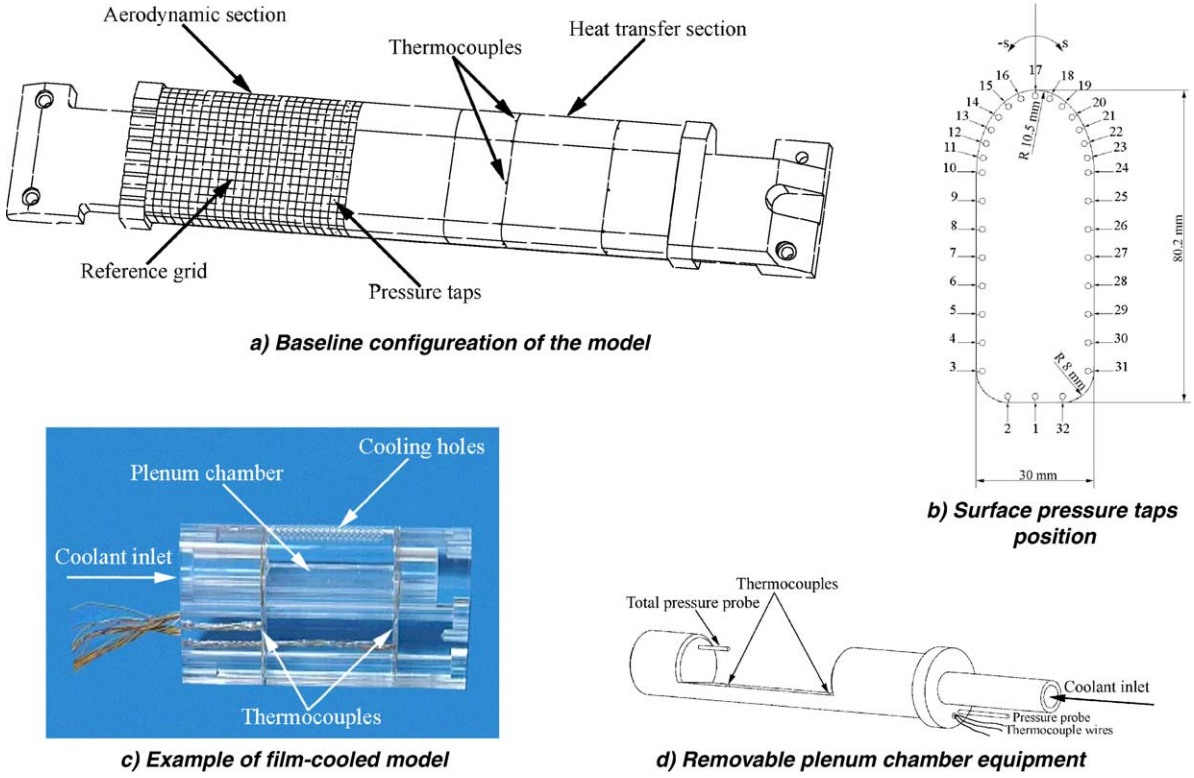

Fig. 2. Mobile assembly instrumentation.

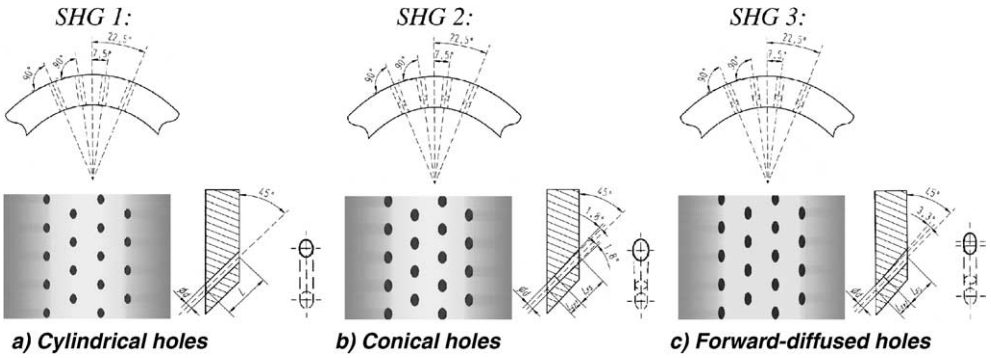

Fig. 3. Showerhead geometries on blunt body models.

Table 1
Geometrical parameters describing the showerhead configurations for the blunt body models

		SHG1	SHG2	SHG3
Diameter ratio	d/D	0.033	0.033	0.033
Exit location angles [°]	γ	±22.5/±7.5	±22.5/±7.5	±22.5/±7.5
Spanwise pitch	p/d	4	4	4
Hole length	L/d	6	6	6
Streamwise inclination angle [°]	φ	90	90	90
Spanwise inclination angle [°]	β	45	45	45
Area ratio		1	1.5	1.26
Exit shape		Cylindrical	Conical	Forward-diffused

or aerodynamic side—has been removed to clarify the view. The ''aerodynamic sidewall'' is equipped with a series of static pressure taps placed up- and downstream of the center blunt body. The first row of pressure taps is used to characterize the incoming flow. Further static pressure taps are distributed around the center blunt body (see Fig. 2b). The information obtained with these pressure taps can be used as upstream boundary condition for CFD analysis.

In order to optimize the optical access, five windows are placed around the insertion passage on the ''heat transfer'' disc. The liquid crystal coating is observed with four miniature color CCD cameras situated behind the Plexiglas windows viewing both sides of the model surface. Halogen light sources and fiber optics are used for homogeneous illumination. The blunt body is situated in the middle of the test section. Since the distance between the stagnation point of the model and the sidewalls is about 8 times the leading edge diameter ($D = 21$ mm), the influence of the sidewalls on the flow developing around the blunt body can be neglected. The mobile assembly and its instrumentation are shown in Fig. 2. It is composed of several aluminum and Plexiglas parts. Aerodynamic measurements are obtained along the aluminum part using 32 static pressure taps (Fig. 2b). Temperature measurements are obtained along the Plexiglas part using 10 embedded thermocouples which assess the preconditioning temperature of the model.

The baseline configuration of the model—heat transfer test section without film cooling holes—is represented in Fig. 2a. The blunt body is equipped with a 135 mm exchangeable part carrying the cooling scheme to be tested (Fig. 2c). This part is coated with 30.5 °C narrow-band reacting liquid crystals. All rows are fed from a single plenum chamber. The plenum chamber is equipped by a removable part holding two thermocouples and a total pressure probe. The coolant is supplied via a Plexiglas tube directly connected to this part. In order to assure repetitive acquisitions of transient coolant gas conditions, this removable plenum chamber instrumentation has been employed for all film-cooled configurations.

2.2. Measurement technique and data reduction

The transient liquid crystal technique is a very commonly used measurement technique for obtaining precise heat transfer data. It consists of monitoring the evolution of the surface temperature—triggered by a heat step. With regards to the measurements presented herein, the heat step is generated by rapidly exposing the preconditioned cold model (preconditioned to about 0 °C) into a hot main flow (typically in the order of 55 °C). During the transient experiment, the color variation of the liquid crystal signal is captured with color CCD cameras. During the measurement phase, each camera view is independently recorded using the standard digital video (DV) format. The data reduction is finally performed using the image processing software developed by Vogel [15]. For the present investigations, air has been used as coolant, resulting in density ratios of about DR = 1.15 to 1.18 for all tests.

For the baseline case (without film cooling), the heat transfer coefficient h can be obtained from the following transcendental equation

$$\frac{T_w - T_{initial}}{T_g - T_{initial}} = \left[1 - \exp\left(\frac{h\sqrt{t}}{\sqrt{k\rho c_p}}\right)^2 \operatorname{erfc}\left(\frac{h\sqrt{t}}{\sqrt{k\rho c_p}}\right)\right] \quad (1)$$

The underlying assumptions of Eq. (1) are that the wall of the test model can be treated as a semi-infinite body and that the heat conduction in this body can be considered to be one-dimensional. These assumptions are well justified

in the present tests. For the case with film cooling, the heat transfer coefficient, defined by

$$q = h_f(T_{aw} - T_w) \tag{2}$$

as well as the adiabatic film cooling effectiveness, defined by

$$\eta = \frac{T_{aw} - T_{rg}}{T_{tc} - T_{tg}} \tag{3}$$

can be obtained by multiple regression analysis from several tests. The reader is referred to [15,16] for a more detailed explanation of this measurement method. The heat transfer coefficient is presented mostly in dimensionless form by

$$\frac{Nu_D}{Re_D^{0.5}} = \frac{hD}{k} \Big/ \left(\frac{u_\infty D}{v}\right)^{0.5}$$

where the Nusselt number Nu_D is divided by $Re_D^{0.5}$.

The data reduction of the liquid crystal signal is performed on a personal computer using an in-house program called DIPS (Digital Image Processing System). A comprehensive description of the program is given in [15].

2.3. Measurement uncertainty

The uncertainties in the measurement of the initial temperature, the wall temperature and the flow temperature are about 0.75 K, 0.2 K and 0.15 K. The uncertainty in the detection of the liquid crystal apparition time t was about 0.1 s. These uncertainties resulted in an error for the obtained film cooling effectiveness and the heat transfer coefficient. An error analysis as detailed by Ireland [17] has been performed. The uncertainties of the above given quantities together with reasonable uncertainties on the material properties indicated a maximum relative error on the obtained heat transfer coefficient of 7%, whereas the maximum absolute error in the film cooling effectiveness was about 0.05.

3. Results

3.1. Aerodynamic results for the blunt body

Before conducting heat transfer and film cooling tests, it was necessary to characterize the aerodynamic flow field in the linear test facility, and to check the alignment of the model within the channel. Three different mainstream flow conditions were investigated yielding inlet Reynolds numbers $Re_D = u_\infty D/v$ of 0.58E+05 to 1.52E+05 and inlet Mach numbers $M = u_\infty/a$ of 0.14 to 0.36. Inlet and outlet isentropic Mach number distributions were measured with sidewall static pressure taps. Measurements were made at a cross plane located 2.4 (respectively 6.4) leading edge diameters upstream (respectively downstream) of the stagnation point. The inlet and outlet isentropic Mach number distributions are found to be uniform over the entire length of the channel. Special attention was taken to align the model with the main flow, because a small misalignment can cause a significant deviation of the coolant and affect the leading edge cooling. Consequently, the symmetry and periodicity of the flow field developing at the model surface were characterized by various techniques. Surface flow visualizations were conducted on the blunt body by using shear sensitive liquid crystals to determine the stagnation line position, to identify the surface flow pattern, and to verify that the strong surface curvature did not cause flow separation. To quantify the flow symmetry, surface isentropic Mach number distributions were estimated at 40% of the blunt body span. For all investigated conditions, the flow velocities on both sides were superimposed. Excellent symmetry was found for all Reynolds numbers. In order to acquire the complete surface isentropic Mach number distribution over the entire test section, the center part—equipped with a series of circumferential pressure taps—was moved by small increments through the channel. Isentropic velocity distributions are shown in Fig. 4 for different Mach

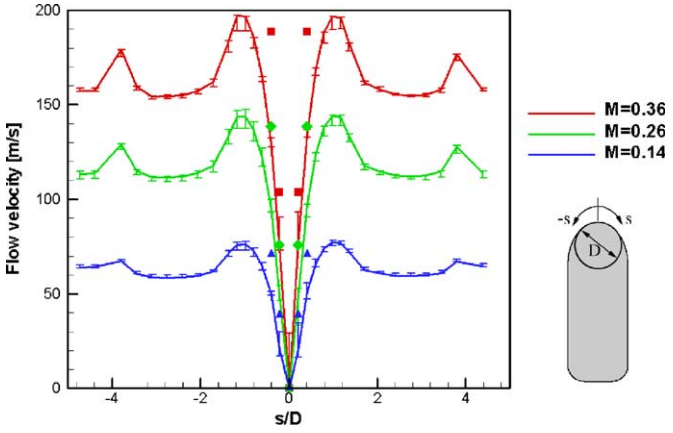

Fig. 4. Isentropic velocity distribution around the blunt body and comparison with the potential flow theory.

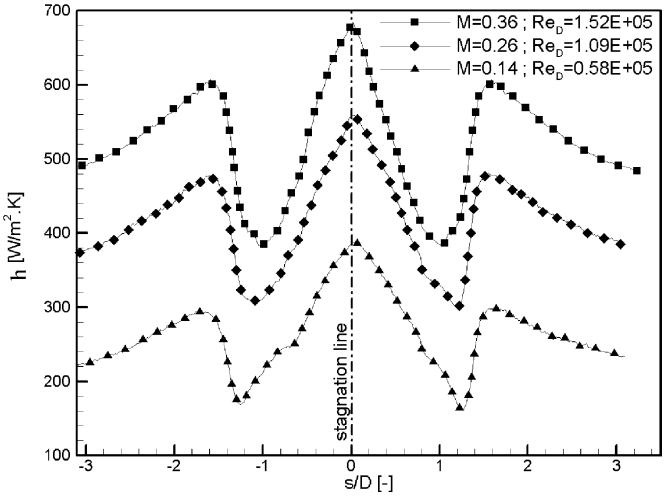

Fig. 5. Baseline heat transfer (without film cooling).

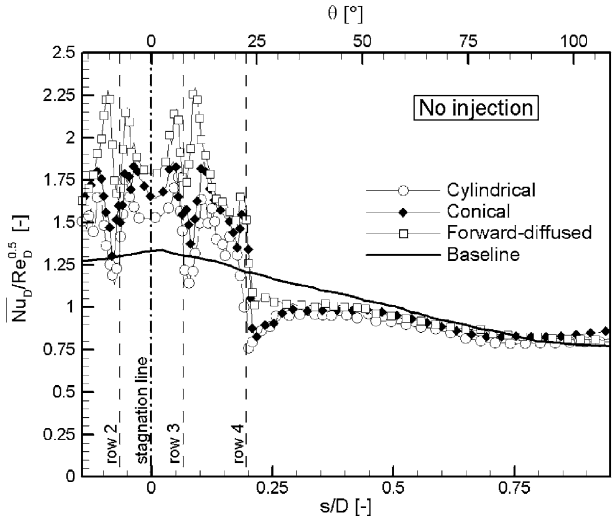

Fig. 6. Effect of the cooling holes on the local heat transfer (no injection, plenum sealed).

numbers. The thick lines indicate the velocities obtained in the middle of the channel, and the error bars mark the maximum variations along the test section. Here, the surface coordinate s is used, which has its origin at the position of the stagnation line of the profile. The flow exhibits an excellent periodicity along the entire length of the test section. For comparison, calculated flow velocities based on the potential theory were superimposed (solid symbols). These theoretical calculations were only made in the front part of the blunt body. Agreement between theory and measurement improves with proximity towards the stagnation point.

3.2. Heat transfer results for the baseline configuration (without film cooling)

In a next step, heat transfer measurements were performed for the baseline case of the blunt body, without film cooling. The spanwise averaged heat transfer coefficients are shown for three different investigated Mach numbers in Fig. 5. Again, the nice symmetry around the stagnation point can be observed. In addition, the high heat transfer near the stagnation point is clearly visible. It can also be seen that the transition point moves upstream with increasing Reynolds numbers.

Introducing the film cooling holes into the test model will change the position of transition on the blunt body and also the heat transfer, even if no cooling flow is injected from the holes. This can be seen in Fig. 6, where experiments are shown for the different tested hole geometries. The results in Fig. 6 indicate that the presence of a film cooling row alone provokes a transition of the boundary layer which, in turn, leads to a strongly enhanced heat transfer immediately behind the injection location. In addition, the cooling hole exit geometry plays a significant role on the heat transfer increase. The heat transfer coefficients

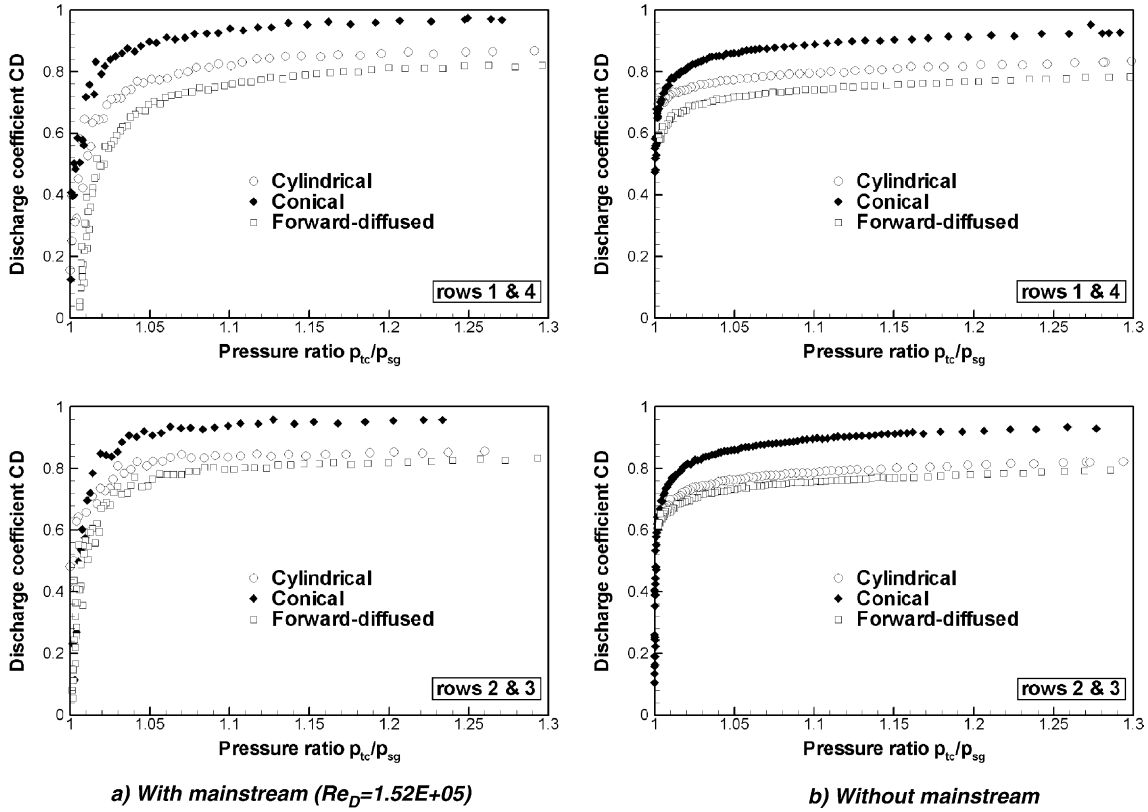

Fig. 7. Comparison of discharge coefficients for fan-shaped and cylindrical holes.

obtained after the first row of holes ($s/D = 0.1$) are 20%, 40%, and 80% higher than for the baseline case considering cylindrical, conical and forward-diffused holes, respectively.

3.3. Results with film cooling

The test program for the film cooling measurements consists of a systematic variation of the blowing rates (from $G = 0.4$ to 1.4) at constant main flow conditions ($Re_D = 1.52\text{E}{+}05$, $M = 0.36$) for three different showerhead configurations and a density ratio DR of about 1.15 to 1.18. The test program was defined in order to be close to engine-like conditions and to cover a realistic range of injection rates. The discharge coefficients ($\text{CD} = \dot{m}/\dot{m}_{\text{ideal}}$) for all hole configurations have been measured. The discharge coefficients of the fan-shaped holes were compared to those measured for cylindrical holes, with and without the influence of the outside main gas flow (Fig. 7). On the one hand, the discharge coefficients for the forward-diffused holes were found to be very close to the values measured for the cylindrical holes, especially for the central rows (rows #2 & #3 at $-7.5°$ and $+7.5°$). On the other hand, the CD values increased by 20% for conical holes compared to the cylindrical holes, with and without the influence of the external flow developing around the blunt body. In their investigation, Hay and Lampard [19] had already reported that conically flared holes show higher CD values than cylindrical holes, provided that the cylindrical inlet to the flare was sufficiently long (two hole

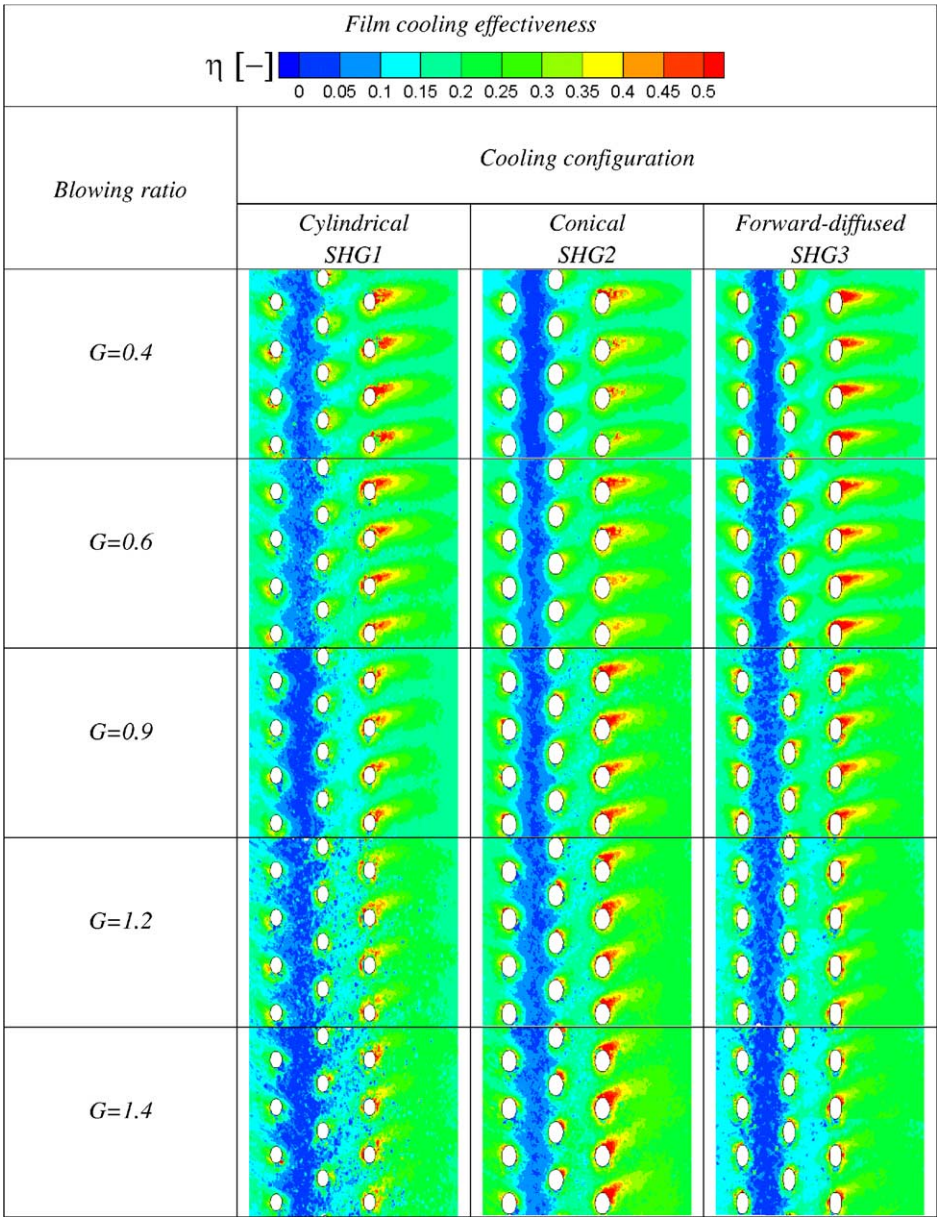

Fig. 8. Detailed film cooling effectiveness on blunt body models at nominal operating point ($Re_D = 1.52\text{E}{+}05$, $M = 0.36$) with varied blowing rates.

diameters at least), which was the case for the present tests. For a more detailed discussion of the CD values, the reader is referred to [16].

The film cooling effectiveness and non-dimensional heat transfer coefficient were evaluated along the surface with the transient liquid crystal technique. For all showerhead injection geometries, detailed distributions of the film cooling performances are presented within the holes pattern in Figs. 8 and 9 revealing information on the lateral and longitudinal film coverage. The contour plots shown in Figs. 8 and 9 represent a portion of the unwrapped model surface covering surface angles (θ) from approximately $-15°$ to 50° and a spanwise distance corresponding to 4 hole spacings. The cooling rows located at $-7.5°$, $+7.5°$ and 22.5° can be seen from the left to the right, and are referred to as rows #2, #3 and #4, respectively. Row #1 is located at $-22.5°$ and is not shown on the plots. The hole exits are represented in full scale for all geometries in order to ease comparisons. The increase of effective exit area for fan-shaped holes is clearly noticeable. Figs. 8 and 9 exhibit an excellent periodicity of the contours in the spanwise direction indicating a homogenous coolant distribution through the cooling holes of the same row.

With regards to the film cooling effectiveness, the presence of pronounced streaks immediately behind row #4—compared to rows #2 and #3—illustrate the fact that the quantity of coolant ejected through the cooling holes of a row depends on its position. In other words, the individual blowing ratio varies over all cooling rows (see also Fig. 10). In fact, the static pressure acting on the hole exits located

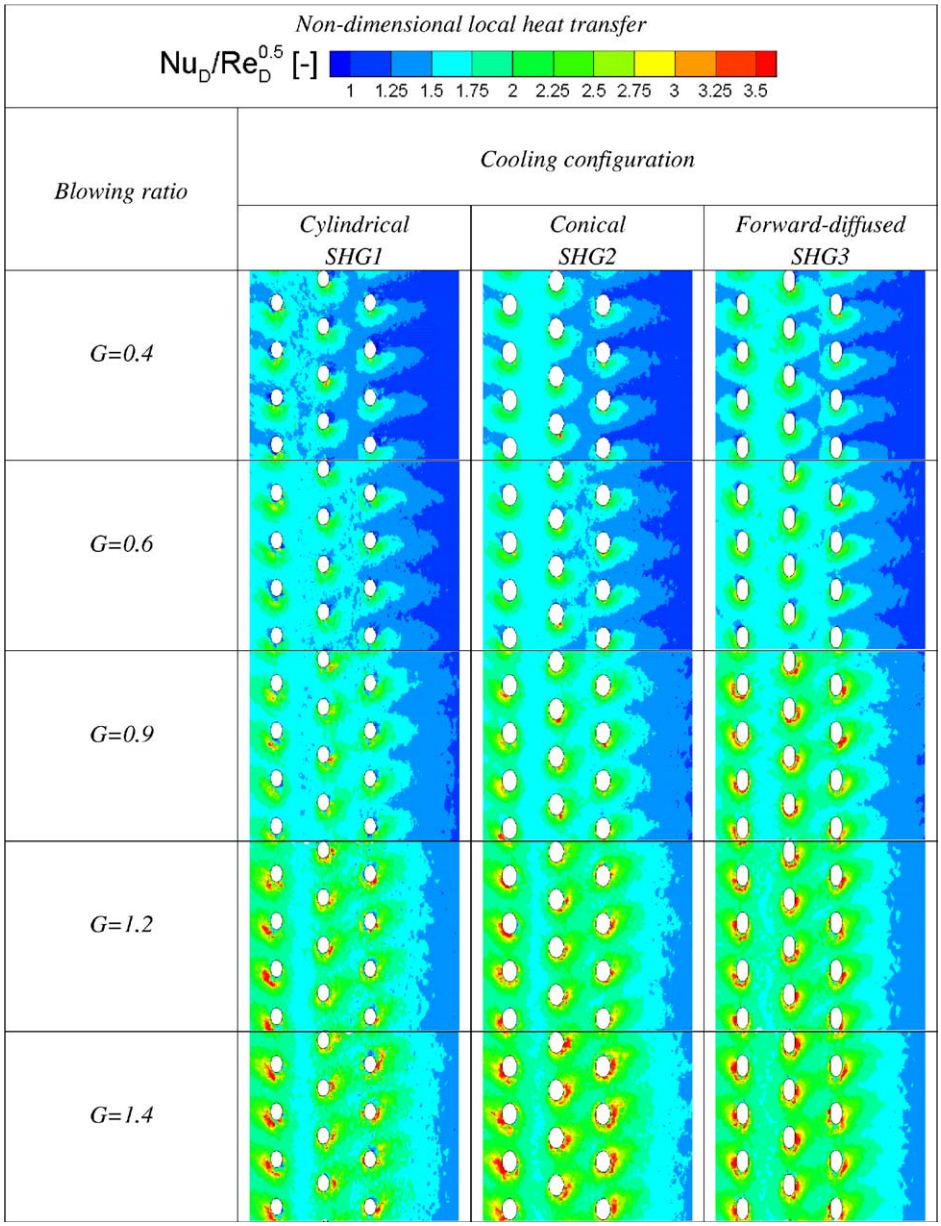

Fig. 9. Detailed heat transfer coefficients on blunt body models at nominal operating point ($Re_D = 1.52E+05$, $M = 0.36$) with varied blowing rates.

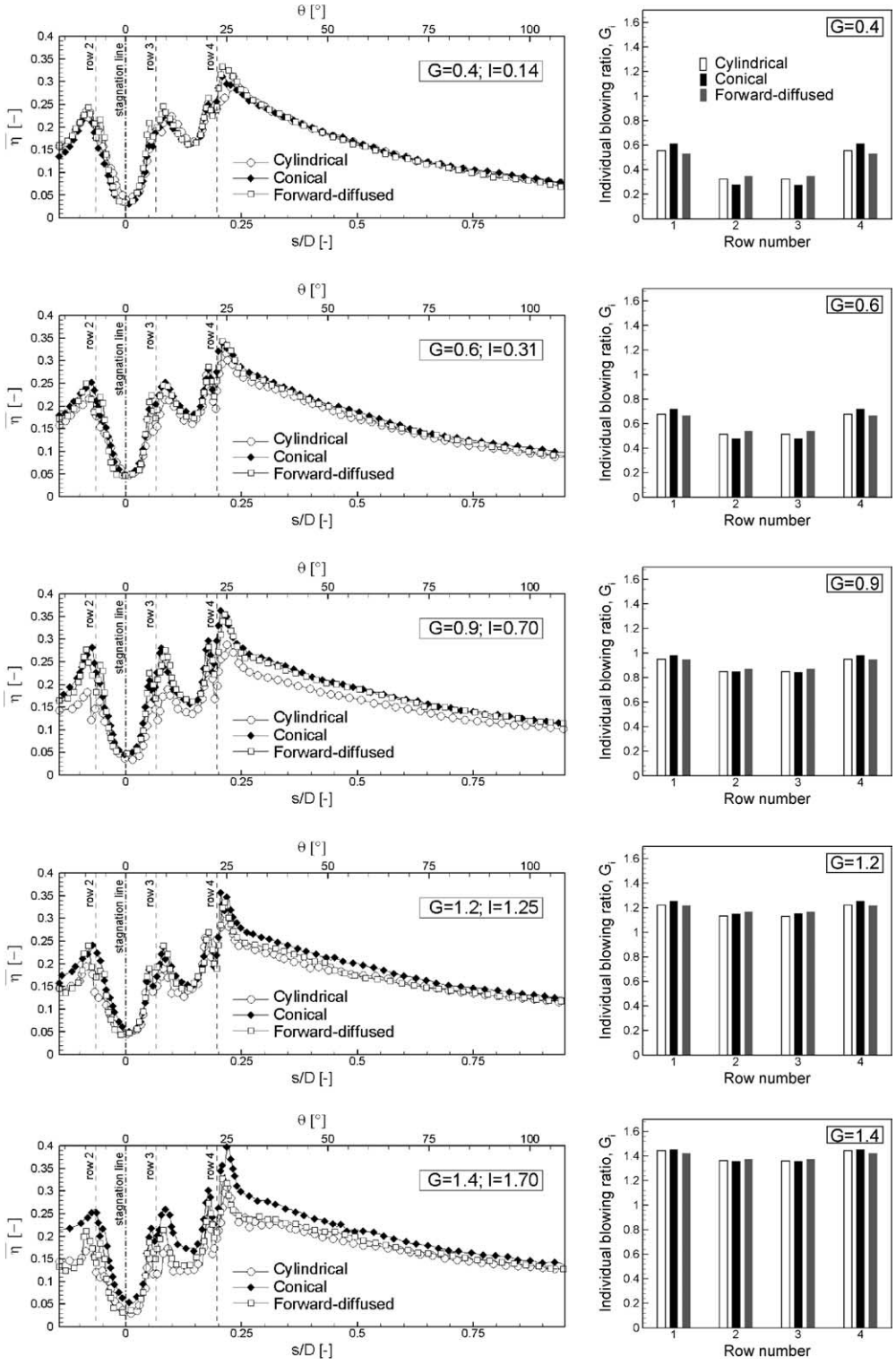

Fig. 10. Comparison of 3 showerhead configurations: spanwise-averaged film cooling effectiveness and individual blowing ratio distributions.

at ±22.5° is lower, so that the coolant mass flow out of these rows is always higher compared to the holes located at ±7.5°. Additionally, the hole shape and the value of the blowing ratio affect the coolant ejection. For the cylindrical holes (SHG1), large streaks, leading to a good film coverage, can be observed behind rows #3 and #4 at low to moderate blowing ratios, and disappear for $G \geqslant 1.2$. This phenomenon has been widely described in the literature and is known as jet "lift-off". The conical holes (SHG2) generate the largest streaks behind rows #3 and #4 at low G. With increasing blowing ratio, the jet mixing process begins, leading to a better lateral film coverage. In

fact, the increased cross-sectional area at the hole exit—compared to a standard cylindrical hole—leads to a reduction of the jet penetration into the main flow, resulting in an increased film cooling effectiveness. Furthermore, the lateral expansion of the hole provides an improved lateral spreading of the jet, leading to a better coverage of the blunt body surface in the spanwise direction. Combining Fig. 8 with 9 it appears that the zones of high film cooling effectiveness correspond to areas of high heat transfer coefficients. This is primarily due to the presence of the cooling holes, and is reinforced by the coolant injection process, both provoking disturbances on the boundary layer. For some cases, peak values up to 3.5 occur close to the holes.

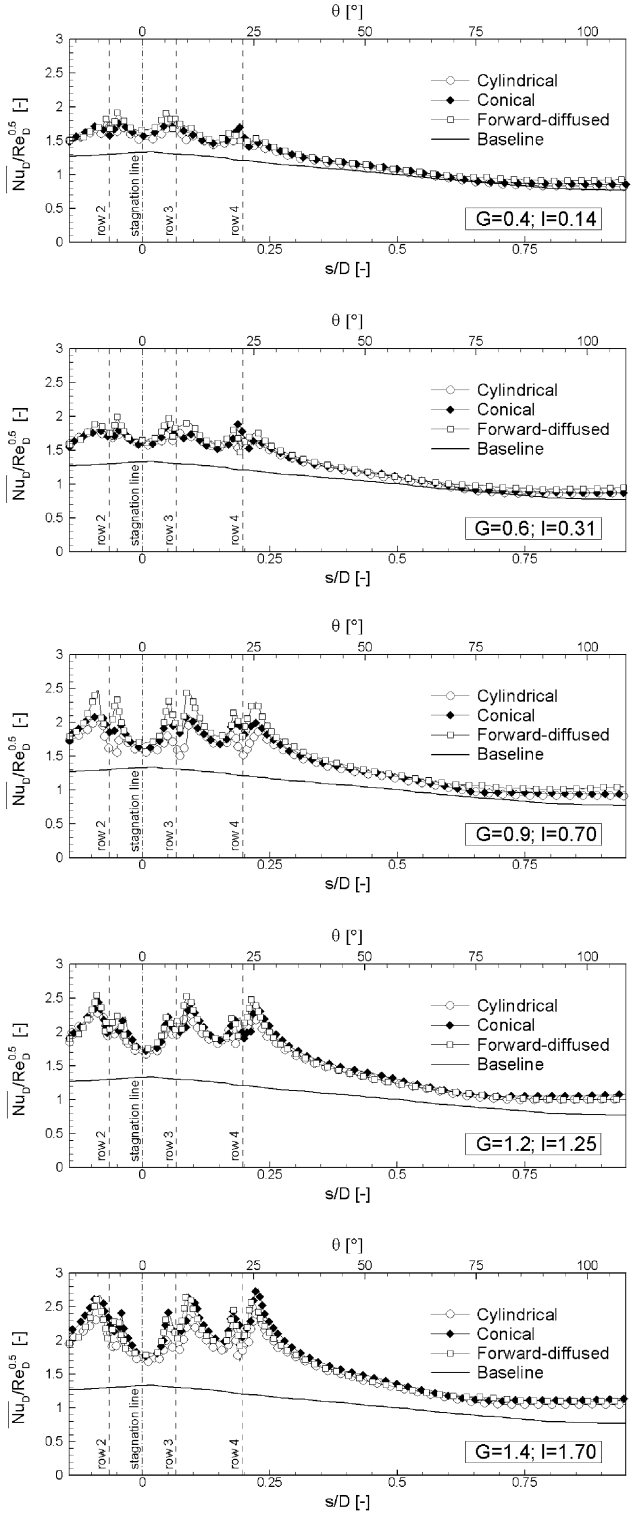

Fig. 11. Comparison of 3 showerhead configurations: non-dimensional heat transfer coefficient distributions.

The spanwise-averaged results ($\bar{\eta}$ and $\overline{Nu_D}/Re_D^{0.5}$), which are derived from the detailed results by integrating the primary quantities in the spanwise direction (from hole to hole), are given over the front part of the blunt body in Figs. 10 and 11. Referring to Fig. 10, the conical holes exhibit the highest $\bar{\eta}$ values downstream of the injection rows, especially with increasing blowing ratios. This trend may be explained looking at the individual blowing ratio distributions. In fact, the quantity of coolant exiting rows #1 and #4 is more significant for the conical holes than for the other geometries. Therefore, rows #1 and #4 provide surface protection when the upstream coolant injection from rows #2 and #3 has lost its cooling capacity. Looking at the spanwise-averaged heat transfer coefficients, it can be seen that the average level of $\overline{Nu_D}/Re_D^{0.5}$ is between 1.5 and 2.5 depending on the blowing ratio and the hole geometry. Downstream of the actual showerhead ($\theta > 35°$, $s/D > 0.3$), the differences between the three cooling configurations are rather small compared to those that affect the film cooling effectiveness measurements. Further downstream of the injection rows ($\theta > 60°$, $s/D > 0.5$), the Nusselt number reaches the same level as the one measured for the baseline case.

4. Conclusions

The present study focused on showerhead cooling performance for gas turbine blade applications. From the experimental results shown in the present paper, the following main conclusions might be drawn:

- The aerodynamic flow field in the linear test facility showed a perfect two-dimensional flow field around the stagnation point.
- Baseline heat transfer measurements were carried out on the blunt body model at various flow conditions: the heat transfer coefficient increases with increasing approach Mach and Reynolds number.
- Inserting cooling holes leads to early transition of the flow at the blunt body and therefore to heat transfer augmentation, even so no coolant is injected.
- The fan-shaped hole configurations showed a better lateral coverage. The best spanwise-averaged film cooling effectiveness was achieved by the conical holes over the widest range of blowing ratios.

Summarizing, it can be noted that the present data consists of very detailed experimental results on aerodynamics and heat transfer for a blunt body with and without showerhead cooling.

Acknowledgements

The LTT kindly acknowledges the financial support of the present project by ALSTOM Power Switzerland. Furthermore, we would like to acknowledge the fruitful discussions with Prof. A. Bölcs (LTT, EPFL), Prof. J. von Wolfersdorf (ITLR, University of Stuttgart) and Dr. S. Parneix (ALSTOM Power Switzerland) concerning various aspects of this project.

References

[1] R.J. Goldstein, Film Cooling, in: T.F. Irvine, J.P. Hartnett (Eds.), Advances in Heat Transfer, vol. 7, Academic Press, New York, 1971, pp. 321–379.
[2] VKI Lecture Series, Film cooling and turbine blade heat transfer, VKI-LS 82-02, 1982.
[3] A.I. Leontiev, Heat and mass transfer problems for film cooling, J. Heat Transfer 121 (1999) 509–527.
[4] G.J. Hanus, M.R. L'Ecuyer, Leading-edge injection for film cooling of turbine vanes, J. Energy 1 (1977) 44–49.
[5] D.W. Luckey, M.R. L'Ecuyer, Stagnation region gas film cooling—Spanwise angled injection from multiple rows of holes, NASA Contr. Rep. 165333, 1981.
[6] A.R. Wadia, D.A. Nealy, Experimental simulation of turbine airfoil leading edge film cooling, J. Turbomach. 110 (1988) 226–232.
[7] W.J. Mick, R.E. Mayle, Stagnation film cooling and heat transfer including its effect within the hole pattern, J. Turbomach. 110 (1988) 66–72.
[8] A.B. Mehendale, J.C. Han, Influence of high mainstream turbulence on leading edge film cooling heat transfer, J. Turbomach. 114 (1992) 707–715.
[9] S. Ou, A.B. Mehendale, J.C. Han, Influence of high mainstream turbulence on leading edge film cooling heat transfer: effect of film hole row location, J. Turbomach. 114 (1992) 716–723.
[10] A. Hoffs, U. Drost, A. Bölcs, An investigation of effectiveness and heat transfer on a showerhead-cooled cylinder, ASME IGTI Conference 97-GT-069, 1997.
[11] S.V. Ekkad, J.C. Han, H. Du, Detailed film cooling measurements on a cylindrical leading edge model: effect of free-stream turbulence and coolant density, J. Turbomach. 120 (1998) 799–807.
[12] H. Reiss, A. Bölcs, Experimental study of showerhead cooling on a cylinder comparing several configurations using cylindrical and shaped holes, J. Turbomach. 122 (2000) 161–169.
[13] I.N. Bronstein, K.A. Semendjajew, Taschenbuch der Mathematik, V. Nauka, Moskau, 1989, 3-322-00259-4.
[14] H. Reiss, Experimental study on film cooling of gas turbine airfoils using shaped holes. Ph.D. Thesis No. 2209, EPFL, 2000.
[15] G. Vogel, Experimental study on a heavy film cooled nozzle guide vane with contoured platforms. Ph.D. Thesis No. 2602, EPFL, 2002.
[16] C. Falcoz, A comparative study of showerhead cooling performance, Ph.D. Thesis No. 2735, EPFL, 2003.
[17] P.T. Ireland, Heat Transfer in Gasturbines, Ph.D. Thesis, Oxford Univ., 1987.
[18] C. Falcoz, B. Weigand, P. Ott, A comparative study on showerhead cooling performance. Int. J. Heat Mass Transfer., accepted for publication.
[19] N. Hay, D. Lampard, The discharge coefficient of flared film cooling holes. ASME paper 95-GT-15, 1995.